from one another by $\sim E_{\rm tot}/mc^2$ in the neighbourhood of the *K*-absorption edge of niobium in the compound lithium niobate.

Further theoretical objections have been made by Creagh (1984) and Smith (1987), who has shown that the Stibius-Jensen correction is not valid, and that, when higher-order multipolar expansions and retardation are considered, the total self-energy correction becomes $E_{\rm tot}/mc^2$ rather than $\frac{5}{3}E_{\rm tot}/mc^2$. Fig. 4.2.6.1 shows the variation of the self-energy correction with atomic number for the modified form factor (Creagh, 1984; Smith, 1987; Cromer & Liberman, 1970).

For the imaginary part of the dispersion correction $f''(\omega, 0)$, which depends on the calculation of the photoelectric scattering cross section, better agreement is found between theoretical results and experimental data. Details of this comparison have been given elsewhere (Section 4.2.4). Suffice it to say that Creagh & Hubbell (1990), in reporting the results of the IUCr X-ray Attenuation Project, could find no rational basis for preferring the Scofield (1973) Hartree–Fock calculations to the Cromer & Liberman (1970, 1981) and Storm & Israel (1970) Dirac–Hartree–Fock–Slater calculations.

Computer programs based on the Cromer & Liberman program (Cromer & Liberman, 1983) are in use at all the major synchrotron-radiation laboratories. Many other laboratories have also acquired copies of their program. This program must be modified to remove the incorrect Stibius–Jensen correction term, and, as will be seen later, the energy term should be modified to be $E_{\rm tot}/mc^2$.

Table 4.2.6.1. *Values of E_{tot}/mc^2 listed as a function of atomic number Z*

Z	Symbol	$E_{\rm tot}/mc^2$
3	Li	−0.0004
4	Be	−0.0006
5	B	−0.0012
6	C	−0.0018
7	N	−0.0030
8	O	−0.0042
9	F	−0.0054
10	Ne	−0.0066
11	Na	−0.0084
12	Mg	−0.0110
13	Al	−0.0125
14	Si	−0.0158
15	P	−0.0180
16	S	−0.0210
17	Cl	−0.0250
18	Ar	−0.0285
19	K	−0.0320
20	Ca	−0.0362
21	Sc	−0.0410
22	Ti	−0.0460
23	V	−0.0510
24	Cr	−0.0560
25	Mn	−0.0616
26	Fe	−0.0680
27	Co	−0.0740
28	Ni	−0.0815
29	Cu	−0.0878
30	Zn	−0.0960
31	Ga	−0.104
32	Ge	−0.114
33	As	−0.120
34	Se	−0.132
35	Br	−0.141
36	Kr	−0.150
37	Rb	−0.159
38	Sr	−0.171
39	Y	−0.180
40	Zr	−0.192
41	Nb	−0.204
42	Mo	−0.216
43	Tc	−0.228
44	Ru	−0.246
45	Rh	−0.258
46	Pd	−0.270
47	Ag	−0.285
48	Cd	−0.300
49	In	−0.318
50	Sn	−0.330
51	Sb	−0.348
52	Te	−0.363
53	I	−0.384
54	Xe	−0.396
55	Cs	−0.414
56	Ba	−0.438
57	La	−0.456
58	Ce	−0.474
59	Pr	−0.492
60	Nd	−0.516
61	Pm	−0.534
62	Sm	−0.558
63	Eu	−0.582
64	Gd	−0.610
65	Tb	−0.624
66	Dy	−0.648
67	Ho	−0.672
68	Er	−0.696
69	Tm	−0.723
70	Yb	−0.750
71	Lu	−0.780
72	Hf	−0.804
73	Ta	−0.834
74	W	−0.864
75	Re	−0.900
76	Os	−0.919
77	Ir	−0.948
78	Pt	−0.984
79	Au	−1.014
80	Hg	−1.046
81	Tl	−1.080
82	Pb	−1.116
83	Bi	−1.149
84	Po	−1.189
85	At	−1.224
86	Rn	−1.260
87	Fr	−1.296
88	Ra	−1.332
89	Ac	−1.374
90	Th	−1.416
91	Pa	−1.458
92	U	−1.470
93	Np	−1.536
94	Pu	−1.584
95	Am	−1.626
96	Cm	−1.669
97	Bk	−1.716
98	Cf	−1.764

4.2.6.2.3.2. *The scattering matrix formalism*

Kissel, Pratt & Roy (1980) have developed a computer program based on the second-order *S*-matrix formalism suggested by Brown, Peierls & Woodward (1955). Their aim was to provide a prescription for the accurate (∼1%) prediction of the total-atom Rayleigh scattering amplitudes.

Their model treats the elastic scattering as the sum of bound electron, nuclear, and Delbrück scattering cross sections, and treats the Rayleigh scattering by considering second-order, single-electron transitions from electrons bound in a relativistic, self-consistent, central potential. This potential was a Dirac–Hartree–Fock–Slater potential, and exchange was included by use of the Kohn & Sham (1965) exchange model. They omitted radiative corrections.

In principle, the observables in an elastic scattering process are momentum ($\hbar\mathbf{k}$) and polarization $\boldsymbol{\varepsilon}$. The complex polarization vectors $\boldsymbol{\varepsilon}$ satisfy the conditions

$$\boldsymbol{\varepsilon}^* \cdot \boldsymbol{\varepsilon} = 1'; \quad \boldsymbol{\varepsilon} \cdot \mathbf{k} = 0. \tag{4.2.6.29}$$

In quantum mechanics, elastic scattering is described in terms of a differential scattering amplitude, M, which is related to the elastic cross section by equation (4.2.6.16).

If polarization is not an observable, then the expression for the differential scattering cross section takes the form of equation (4.2.6.17). If polarization is taken into account, as may be the case when a polarizer is used on a beam scattered from a sample irradiated by the linearly polarized beam from a synchrotron-radiation source, the full equation, and not equation (4.2.6.17), must be used to compute the differential scattering cross section.

The principle of causality implies that the forward-scattering amplitude $M(\omega, 0)$ should be analytic in the upper half of the ω plane, and that the dispersion relation

$$\text{Re } M(\omega, 0) = \frac{2\omega^2}{\pi} \int_0^\infty \frac{\text{Im } M(\omega', 0)}{\omega'(\omega'^2 - \omega^2)} \text{d}\omega' \tag{4.2.6.30}$$

should hold, with the consequence that

$$\text{Re } M(\infty, 0) = -\frac{2}{\pi} \int_0^\infty \frac{\text{Im } M(\omega', 0)}{\omega'} \text{d}\omega'. \tag{4.2.6.31}$$

This may be rewritten as

$$M(\omega, 0) - M(\infty, 0) = f'(\omega, 0) + if''(\omega, 0), \qquad (4.2.6.32)$$

with the value of $f'(\omega, 0)$ defined by equation (4.2.6.15). Using the conservation of probability,

$$\text{Im } M(\omega, 0) = \frac{\omega}{4\pi r_e c}\sigma_{\text{tot}}, \qquad (4.2.6.33)$$

which is to be compared with equation (4.2.6.23).

Starting with Furry's extension of the formalism of quantum mechanics proposed by Feynman and Dyson, the total Rayleigh amplitude may be written as

$$M_n = \sum_p \left[\frac{\langle n|T_1^*|p\rangle\langle p|T_1|n\rangle}{E_n - E_p + \hbar\omega} + \frac{\langle n|T_2|p\rangle\langle n|T_2^*|p\rangle}{E_n - E_p + \hbar\omega} \right], \qquad (4.2.6.34)$$

where

$$T_1 = \boldsymbol{\alpha} \cdot \boldsymbol{\varepsilon}_i \cdot \exp(i\mathbf{k}_i \cdot \mathbf{r})$$

and

$$T_2 = \boldsymbol{\alpha} \cdot \boldsymbol{\varepsilon}_f^* \cdot \exp(-i\mathbf{k}_f \cdot \mathbf{r}).$$

The $|p\rangle$ are the complete set of bound and continuum states in the external field of the atomic potential. Singularities occur at all photon energies that correspond to transitions between bound $|n\rangle$ and bound state $|p\rangle$. These singularities are removed if the finite widths of these states are considered, and the energies E are replaced by $iE\Gamma/2$, where Γ is the total (radiative plus non-radiative) width of the state (Gavrila, 1981). By use of the formalism suggested by Brown *et al.* (1955), it is possible to reduce the numerical problems to one-dimensional radial integrals and differential equations. The required multipole expansions of T_1 and the specification of the radial perturbed orbitals that are characterized by angular-momentum quantum numbers have been discussed by Kissel (1977). Ultimately, all the angular dependence on the photon scattering angle is written in terms of the associated Legendre functions, and all the energy dependence is in terms of multipole amplitudes.

Solutions are not found for the inhomogeneous radial wave equations, and Kissel (1977) expressed the solution as the linear sum of two solutions of the homogeneous equation, one of which was regular at the origin and the other regular at infinity.

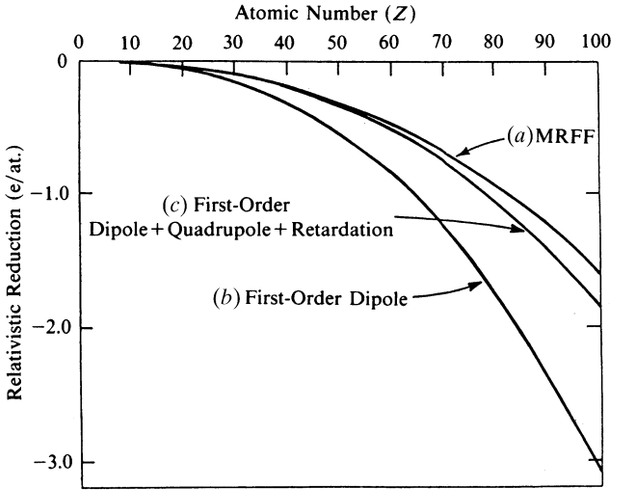

Fig. 4.2.6.1. The relativistic correction in electrons per atom for: (*a*) the modified form-factor approach; (*b*) the relativistic multipole approach; (*c*) the relativistic dipole approach.

Because excessive amounts of computer time are required to use these direct techniques for calculating the amplitudes from all the subshells, simpler methods are usually used for calculating outer-shell amplitudes. Kissel & Pratt (1985) used estimates for outer-shell amplitudes based on the predictions of the modified form-factor approach. A tabulation of the modified relativistic form factors has been given by Schaupp, Schumacher, Smend, Rullhusen & Hubbell (1983).

Because of the generality of their approach, the computer time required for the calculation of the scattering amplitudes for a particular energy is quite long, so that relatively few calculations have been made. Their approach, however, does not confine itself solely to the problem of forward scattering of photons as does the Cromer & Liberman (1970) approach. Using their model, Kissel *et al.* (1980) have been able to show that it is incorrect to assign a dependence of the dispersion corrections on the scattering vector $\boldsymbol{\Delta}$. This is at variance with some established crystallographic practices, in which the dispersion corrections are accorded the same dependence on $\boldsymbol{\Delta}$ as $f_0(\boldsymbol{\Delta})$, and also at

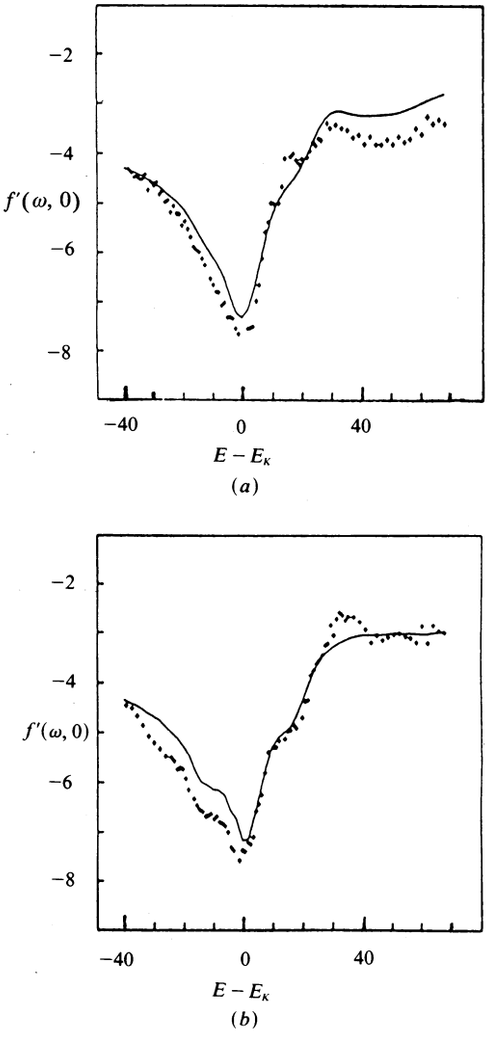

Fig. 4.2.6.2. Measured values of $f'(\omega, 0)$ at the *K*-edge of Nb in $LiNbO_3$ and the Kramers–Kronig transformation of $f''(\omega, 0)$. The curve is obtained by transformation and the points are measured by interferometry. For (*a*), the polarization of the incident radiation is parallel to the hexagonal *c* axis, and for (*b*) it is at right angles to the hexagonal *c* axis. After Bonse & Henning (1986). Note that the distortion of the dispersion curve is due to X-ray absorption near-edge structure (XANES) effects (Section 4.2.4).

variance with the predictions of Wagenfeld's (1975) non-relativistic model.

4.2.6.2.4. *Intercomparison of theories*

A discussion of the validity of the non-relativistic dipole approximation for the calculation of forward Rayleigh scattering amplitudes has been given by Roy & Pratt (1982). They compared their relativistic multipole calculations with the relativistic dipole approximation and with the non-relativistic dipole approximation for two elements, silver and lead. They concluded that a relativistic correction to the form factor of order $(Z\alpha)^2$ persists in the high-energy limit, and that this constant correction accounts for much of the deviation from the non-relativistic dipole approximation at all energies above threshold. In addition, their results illustrate that cancelling occurs amongst the relativistic, retardation, and higher multipole contributions to the scattering amplitude. This implies that care must be taken in assessing where to terminate the series that describes the multipolarity of the scattering process.

In a later paper, Roy, Kissel & Pratt (1983) discussed the elastic photon scattering for small momentum transfers and the validity of the form-factor theories. In this paper, which compares the relativistic modified form factor with experimental results for lead and a relativistic form factor and the tabulation by Hubbell, Veigele, Briggs, Brown, Cromer & Howerton (1975), it is shown that the modified relativistic form-factor approach gives better agreement with experiment for high momentum transfers ($<104\,\text{Å}^{-1}$) than the non-relativistic, form-factor theories.

Kissel *et al*. (1980) used the *S*-matrix technique to calculate the real part of the forward-scattering amplitude $f'(\omega, 0)$ for the inert gases at the wavelength of Mo $K\alpha_1$. These values are compared with the predictions of the relativistic dipole theory (RDP) and the relativistic multipole theory (RMP) in Table 4.2.6.2(*a*). In most cases, the agreement between the *S* matrix and the RMP theory is excellent, considering the differences in the methodology of the two sets of calculations. Table 4.2.6.2(*b*) shows comparisons of the real part of the forward-scattering amplitude $f''(\omega, 0)$ calculated for the atoms aluminium, silicon, zinc, germanium, silver, samarium, tantalum and lead using the approach of Kissel *et al*. (1980) with that of Cromer & Liberman (1970, 1981), with tabulations by Wagenfeld (1975), and with values taken from the tables in this section. Although reasonably satisfactory agreement exists between the relativistic values, large differences exist between the non-relativistic value (Wagenfeld, 1975) and the relativistic values. The major difference between the relativistic values occurs because of differences in estimation of the self-consistent-field term, which is proportional to E_{tot}/mc^2. The Cromer & Liberman (1970) relativistic dipole value is $+\frac{5}{3}(E_{\text{tot}}/mc^2)$, whereas the tabulation in this section uses the relativistic multipole value of $(+E_{\text{tot}}/mc^2)$. This causes a vertical shift of the curve, but does not alter its shape. Should better estimates of the self-energy term be found, the correction is simply that of adding a constant to each value of $f'(\omega, 0)$ for each atomic species. There is a significant discrepancy between the Kissel *et al*. (1980) result for ^{62}Sm and the other theoretical values. This is the only major point of difference, however, and the results are better in accord with the relativistic multipole approach than with the relativistic dipole approach. Note that the relativistic multipole approach does not include the Stibius-Jensen correction, which alters the shape of the curve.

In §4.2.6.3.3, some examples are given to illustrate the extent to which predictions of these theories agree with experimental data for $f'(\omega, 0)$.

That there is little to choose between the different theoretical approaches where the calculation of $f''(\omega, 0)$ is concerned is illustrated in Table 4.2.6.3. In most cases, the agreement between the scattering matrix, relativistic dipole, and relativistic multipole values is within 1%. In contrast, there are some significant differences between the relativistic and the non-relativistic values of $f''(\omega, 0)$. The extent of the discrepancies is greater the higher the atomic number, as one might expect from the assumptions made in the formulation of the non-relativistic model. Some detailed comparisons of theoretical and experimental data for linear attenuation coefficients [proportional to $f''(\omega, 0)$] have been given by Creagh & Hubbell (1987) for silicon, and for copper and carbon by Gerward (1982, 1983). These tend to confirm the assertion that, at the 1% level of accuracy, there is little to choose between the various relativistic models for computing scattering cross sections.

Further discussion of this is given in §4.2.6.3.3.

4.2.6.3. *Modern experimental techniques*

The atomic scattering factor enters directly into expressions for such macroscopic material properties as the *refractive index*, n, and the *linear attenuation coefficient*, μ_l. The refractive index depends on the dielectric susceptibility χ through

$$n = (1 + \chi)^{1/2}, \tag{4.2.6.35}$$

where

$$\chi = -\frac{r_e\lambda^2}{\pi}\sum_j N_j f_j(\omega, \mathbf{\Delta}) \tag{4.2.6.36}$$

and N_j is the number density of atoms of type j.

The imaginary part of the dispersion correction $f''(\omega, \mathbf{\Delta})$ for the case where $\mathbf{\Delta} = 0$ is related to the atomic scattering cross section through equation (4.2.6.23).

Experimental techniques that measure refractive indices or X-ray attenuation coefficients to determine the dispersion corrections involve measurements for which the scattering vector, $\mathbf{\Delta}$, is zero or close to it. Data from these experiments may be compared *directly* with data sets such as Cromer & Liberman (1970, 1981).

Other techniques measure the intensities of Bragg reflections from crystalline materials or the variation of intensities within one particular Laue reflection (*Pendellösung*). For these cases, $\mathbf{\Delta} = g_{hkl}$, the reciprocal-lattice vector for the reflection or reflections measured. These techniques can be compared only indirectly with existing relativistic tabulations, since these have been developed for the $\mathbf{\Delta} = 0$ case. Data are available for elements having atomic numbers less than 20 in the non-relativistic case (Wagenfeld, 1975).

The following sections will discuss some modern techniques for the measurement of dispersion corrections, and an intercomparison will be made between experimental data and theoretical calculations for a representative selection of atoms and at two extremes of photon energies: near to and remote from an absorption edge of those atoms.

4.2.6.3.1. *Determination of the real part of the dispersion correction*: $f'(\omega, 0)$

X-ray interferometer techniques are now used extensively for the measurement of the refractive index of materials and hence

references